Turbulence studies in NBI heated discharges by the Phase Contrast Imaging diagnostic in the Wendelstein 7-X stellarator

Z. Huang[1], E. Edlund[2], M. Porkolab[1], A. von Stechow[3], J-P. Bähner[3], S. K. Hansen[1], O. Grulke[3,4], O. P. Ford[3], M. N. A. Beurskens[3], S. A. Bozhenkov[3], S. Lazerson[3], and the Wendelstein 7-X Team

[1] *MIT Plasma Science and Fusion Center, Cambridge, MA, USA*

[2] *SUNY Cortland, Cortland, NY, USA*

[3] *Max-Planck-Institut für Plasmaphysik, Greifswald, Germany*

[4] *Technical University of Denmark, Kongens Lyngby, Denmark*

Introduction

One of the major optimization criteria of the Wendelstein 7-X (W7-X) stellarator is reduced neoclassical transport compared to classical stellarators [1]. The optimization has been proven to be successful from the experimental results in the first operation phase [2, 3]. As a result, a significant fraction of the transport of heat and particles is dominated by turbulence transport [4]. Turbulence in magnetized plasmas is usually generated by temperature and density gradient driven electrostatic micro-instabilities. Ion-scale turbulence, in particular, ion temperature gradient (ITG) and trapped electron modes (TEM), are suggested by theoretical and gyrokinetic simulation studies to be the primary transport-relevant instabilities in the W7-X core plasma [5, 6], whereas transport by electron-scale instabilities is generally strongly reduced [7].

Fluctuation diagnostics such as phase contrast imaging (PCI) [8, 9, 10] and Doppler backscattering (DBS) have been utilized on W7-X to identify and monitor broadband instabilities. PCI measures line-integrated absolute electron density fluctuations, $I \propto \int n \mathrm{d}l$, along an infra-red laser beam across the W7-X vacuum vessel from inboard to outboard side intersecting the magnetic axis. By imaging the 32 line-of-sights determined by the 32 channels of the detector array, fluctuations are spatially resolved along a roughly poloidal direction. The instrumental lower cutoff is at $k_\mathrm{c} = 1.55$ cm^{-1}, the Nyquist wavenumber ranges from $k_\mathrm{N} = 4$ to 25 cm^{-1} thanks to the flexible magnification of the laser beam, allowing the PCI diagnostic to well resolve ion-scale turbulence such as ITG and TEM with typical W7-X plasma parameters.

Turbulence in standard ECH discharges

Most discharges in the first operation phase of W7-X are gas-fueled and heated by ECH only, without direct ion heating nor additional central fueling such as NBI or pellets. An overview of a typical gas-fueled ECH discharge is shown in Fig. 1. The line-integrated density is kept roughly constant, while the ECH power is reduced periodically during the discharge.

As a result, the central electron temperature T_e and diamagnetic energy W_{dia} decrease during the discharge, while the central T_i remains roughly unchanged. The absolute density fluctuation amplitude measured by PCI is also reduced with the ECH power, as well as the normalized fluctuation amplitude. On the other hand, the energy confinement time τ_E increases with decreasing ECH power. Similarly, it has been found that the impurity transport time increases with decreasing ECH power [11]. The PCI measurements indicate that decreasing turbulence level with ECH power correlates with improved energy and particle confinement. Gyrokinetic simulations also suggest that ITG-type turbulence acts as the main channel of the energy and impurity particle transport, and the negative dependence of the ITG linear growth rate on the T_e/T_i ratio causes the drop in turbulence level with lower ECH power and thus the improved confinement [11].

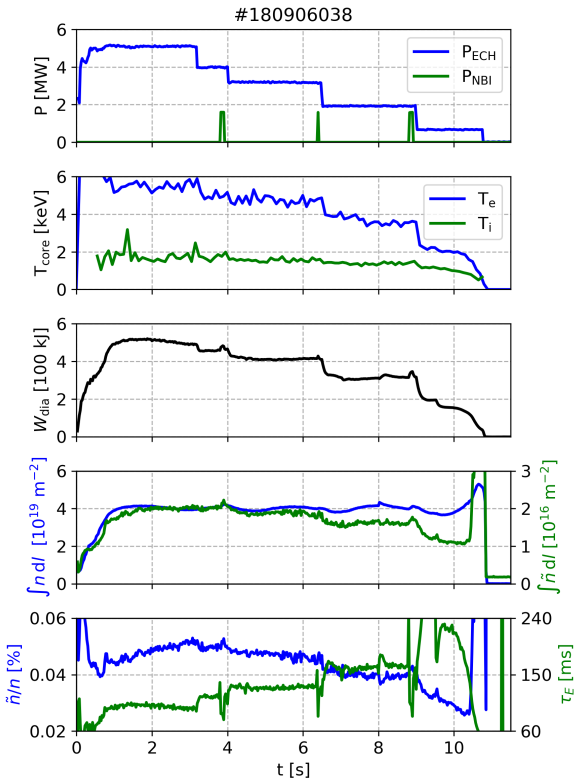

Figure 1: Discharge overview for a typical ECRH discharge in W7-X

Turbulence in pure-NBI discharges

Figure 2 shows the time evolution of a typical pure-NBI discharge. The plasma is initially heated by 2 MW ECH till $t = 1$ s, when the gas fueling stops as well. The central electron temperature drops from 2 to 1 keV when ECH is switched off. At the same time, 3.5 MW NBI is switched on and the plasma is sustained by pure-NBI until $t = 3$ s. The line-integrated plasma density continues to increase during the pure-NBI phase. The diamagnetic energy also increases with constant NBI heating power, resulting in an increasing τ_E. The absolute density fluctuation amplitude measured by PCI features an initial jump during the heat switch, and then it falls back in about 0.5 s and keeps nearly unchanged after, even though the bulk density keeps increasing. As a result, the normalized fluctuation level continues to decrease during the pure-NBI phase.

Figure 3 shows that the central density doubled from 5×10^{19} m^{-3} to 1×10^{20} m^{-3} while the edge plasma density profile outside $r_{eff}/a = 0.5$ remains nearly unchanged, leading to a strongly centrally peaked density profile. This indicates that the density fluctuations measured by PCI are likely originated from the edge plasma, while the turbulence in the core plasma is strongly reduced with the increasing density gradient. However, the temperature in the pure-NBI phase

remains low because the increasing density due to fueling absorbs much of the available NBI power.

The correlation between the peaked density profile and improved confinement has been observed in W7-X ECH plasmas under certain conditions, for example by injecting fueling pellets into the plasma core, or by massive Laser Blow-off to reduce the edge density, thus transiently creating a peaked density profile and improved confinement regimes [12]. Gyrokinetic simulations showed that increased density gradient with peaked profile brings down $\eta_i = \frac{\delta T_i}{T_i} / \frac{\delta n_i}{n_i}$ and thus stabilizes ITG turbulence. While a high density gradient would destabilize TEM turbulence in tokamaks, the maximum-J magnetic geometry of W7-X high-mirror configuration stabilizes TEM turbulence by averaging "good" and "bad" curvature regions along the particle orbit [13].

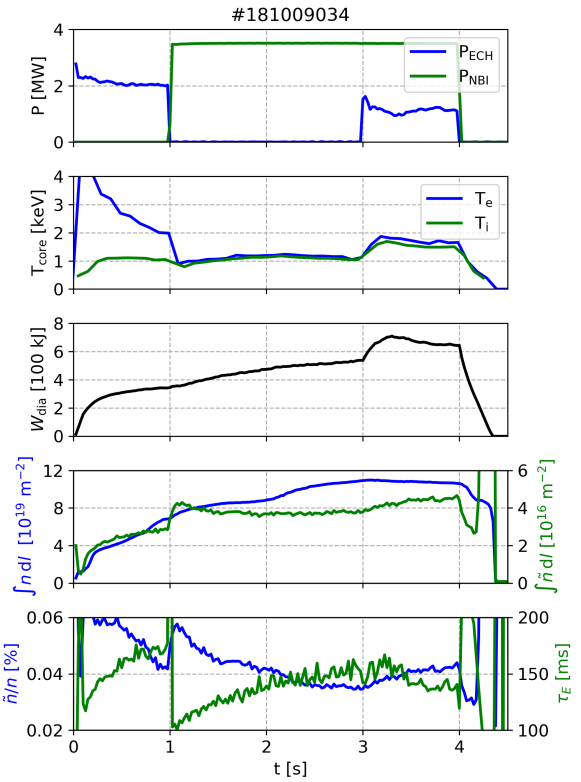

Figure 2: Discharge overview for discharge #20181009.34 in W7-X.

In contrast to other pure-NBI discharges in which the peaked density profile continues to develop till the end of the discharge, in Fig. 2,3 we show what happens when injecting 1 MW ECH power to the pure-NBI plasma after $t = 3$ s. This leads to a fast drop in central plasma density to 8×10^{19} m^{-3} from $t = 3$ to 3.3 s. At the same time, both electron and ion temperature in the core plasma increase from 1 to 1.75 keV, leading to an increase in W_{dia}. On the other hand, the broadband density fluctuation amplitude increases during this time, and τ_{E} starts to decrease. After $t = 3.3$ s, the temperature and diamagnetic energy both fall back to a new state and then remain stable. Figure 3 shows that in this state the density profile is still peaked in the core, roughly the same as $t = 2.2$ s in the pure-NBI phase. However, the additional ECH now provides enough heating power to peak up the ion tem-

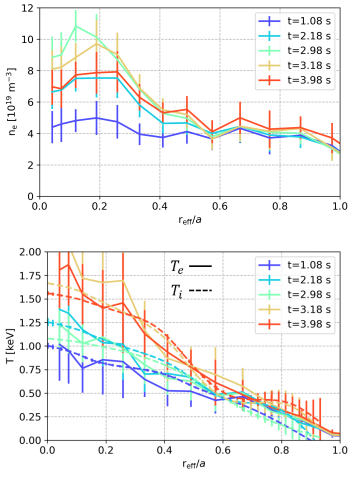

Figure 3: Density (top) and temperature profiles (bottom) for discharge #20181009.34 in W7-X.

perature profile, creating a T_i gradient at around the same radial
location as the density gradient, where η_i is around 1.5. This indeed enhances ITG modes and therefore the confinement slightly deteriorates from the pure-NBI phase, however $\tau_E = 140$ ms is still higher than ≈ 100 ms with similar total input power in the ECH-only discharge.

Conclusion

A highly centrally peaked density profile can be created by pure NBI heating in W7-X. While the central density and diamagnetic energy continues to increase, the absolute density fluctuation amplitude measured by PCI remains surprisingly unchanged, leading to a decreasing relative fluctuation amplitude and increasing confinement time. Adding low power ECH to the pure-NBI plasma slightly increases the turbulence, creates both peaked density and ion temperature profiles and improved confinement comparing to standard ECH discharges. The turbulence measurements are qualitatively consistent with particle and heat transport studies [14].

Acknowledgment

Support for the MIT and SUNY-Cortland participation was provided by the US Department of Energy, Grant DE-SC0014229. This work has been carried out within the framework of the EUROfusion Consortium and has received funding from the Euratom research and training programme 2014-2018 and 2019-2020 under grant agreement number 633053. The views and opinions expressed herein do not necessarily reflect those of the European Commission. S. K. Hansen acknowledges support by an Internationalisation Fellowship (CF19-0738) from the Carlsberg Foundation.

References

[1] G. Grieger, et al., Physics of Fluids B: Plasma Physics **4**, 2081 (1992)
[2] T. Klinger, et al., Nuclear Fusion **59**, 112004 (2019)
[3] R. C. Wolf, et al. 2019 Physics of Plasmas **26**, 082504 (2019)
[4] S. A. Bozhenkov, et al., Nuclear Fusion **60**, 066011 (2019)
[5] J. Proll, et al., Physical Review Letters **108**, 245002 (2012)
[6] P. Xanthopoulos, et al., Physical Review X **6**, 021033 (2016)
[7] G. Plunk, et al., Physical Review Letters **122**, 035002 (2019)
[8] E. Edlund, et al., Review of Scientific Instruments **89**, 10E105 (2018)
[9] Z. Huang, et al., Journal of Instrumentation **14**, P01014 (2021)
[10] J-P. Bähner, et al., accepted by Journal of Plasma Physics (2021)
[11] Th. Wegner, et al., Nuclear Fusion **60**, 124004 (2020)
[12] A. von Stechow, et al., Invited talk, 22nd International Stellarator and Heliotron Workshop 2019 (Madison, WI)
[13] J. Alcuson, et al., Plasma Physics and Controlled Fusion **62** 035005 (2020)
[14] O. P. Ford, et al., 47th EPS conference on plasma physics (2021)